Optical Pumping

Niveditha Ramasubramanian[1] and William Roh[2]

Abstract— **In this experiment, we use the technique of optical pumping to pump Rb^{85} and Rb^{87} into a desired meta-stable state by shining a light of λ = 795nm (D1 line) with σ+ (left hand circularly polarized) helicity. Once we have this state, we caused stimulated emission into lower sub-magnetic and observed resonance due to D1 line. Using the absorption frequency, we determined the Lande g-factor and the ambient magnetic field. We also observed the Zeeman Spectrum by applying high external magnetic field to this Rb cell.**

I. Introduction

Optical pumping is a method in which light of a particular polarization is used to populate electrons into a specific quantum state. In our experiment we use a mixture of ^{87}Rb and ^{85}Rb and light of wavelength 795nm to excite electrons from $5^2S_{1/2}$ state to $5^2P_{1/2}$ state. Figure 1 gives a brief overview of the spliiting of energy levels in ^{87}Rb atom due to various interactions within the atom which can be solved as a pertubation to the main Hamiltonian.

This basic principle of injecting light to excite a medium is highly relevant in modern technology. Most common uses of the optical pump include laser diodes, discharge lamps, dye lasers, and solid-state lasers (used for titanium-sapphire lasers). However this technique has an enormous significance beyond laser production. It is used in precise measurement of atomic hyperfine level splittings, weak magnetic field in biological systems, atomic electron polarization and relaxation rates etc. It is a simple and yet fascinating experiment that can be used to study the interaction between light and matter and some of the basic principles of quantum mechanics, like splitting of energy levels, selection rule, energy-time uncertainty etc.

II. Previous Works

Optical pumping was developed by Alfred Kastler. Collaborating with Jean Brossel, Kastler began quantum mechanics research (light and matter interaction) as well as spectroscopy. In 1950, Kastler presented the idea that electrons - with the help of electromagnetic radiation - could be pumped up to a fixed higher energy and then fall back to fixed lower levels. By working on both optical and magnetic resonance, Kastler developed the method of optical pumping. This allowed for precise determination of energy levels, and was crucial for the completion of laser and maser theory. For his work, Kastler was awarded the Nobel Prize in Physics 1966 "for the discovery and development of optical methods for studying Hertzian resonances in atoms".

III. Theoretical Model

When we consider an atom to be Hydrogen like all states with same value of n, the radial quantum number, have the same energy level. Adding the coulombic interaction between various electrons in the atom causes the degeneracy in orbital quantum number, l, to lift and thus there is an energy difference between $5S$ and $5P$ levels. Adding spin orbit coupling which is the interaction of spin of the electron with its orbital angular momentum causes the $5^2P_{1/2}$ and $5^2P_{3/2}$ to split. Similarly when we include the spin of the nucleus, I, and its interaction with the total angular momentum, J, of the electron, it causes hyper-fine splitting as indicated by quantum number $F = I + J$.

Although there is a small amount of splitting of degenerate M_f levels due to earth's magnetic field, we ignore that for our explanation of optical pumping. When we send circularly polarized light with a certain helicity, say -1, due to conservation of angular momentum. Electrons in $M_f = 2$ get pumped to $M_f = 1$, $M_f = 0$ to $M_f = -1$ etc. But atoms in $M_f = -2$ do not have an energy

level with appropriate angular momentum to get pumped to, thus they remain there in a meta stable state. All electrons in excited state now emit light with any polarization and return to ground state to any M_f. Over time the number of atoms $M_f = -2$ is highly populated and thus we say the atom is Optically pumped.

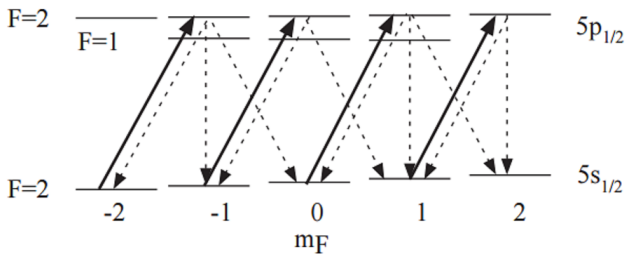

Fig. 1. A schematic layout of submagnetic levels and their allowed transition states when excited by $\sigma+$ light. The solid lines and dashed lines correspond to excitation and de-excitation transition possibilites respectively.

In the presence of external magnetic field, degeneracy in the sub-magnetic levels are lifted. The energy gap between adjacent sub-magnetic level and the external magnetic field is given by

$$\nu = \frac{g_f m_f \mu_b}{h} B \tag{1}$$

Wherein, ν is the frequency corresponding to the energy gap, g_f is the hyper-fine Lande g-factor, μ_b is the Bohr magneton, B is the external magnetic field and h is the Planck's constant.
Under the presence of high external magnetic field, there is no analytic solution for the energy level splitting of the full Hamiltonian given by,

$$H = \frac{\mu_B B_{ext}}{\hbar}(g_s S_z + g_L L_z + g_I I_z) \tag{2}$$

Here, S, L and I refer to the quantum numbers corresponding to electron spin (1/2), orbital angular momentum and spin of the nucleus (5/2 for ^{85}Rb and 3/2 for ^{87}Rb). This Hamiltonian is numerically diagonalized and it's solution is given by the Breit-Wigner formula.

$$\Delta E_{I,m_I,m_j} = -\frac{\Delta E_{HF}}{2(2I+1)} + g_I \mu_B m B_{ext} \pm \frac{\Delta E_{HF}}{2}\left(1 + \frac{4mx}{2I+1} + x^2\right) \tag{3}$$

IV. Experimental Setup

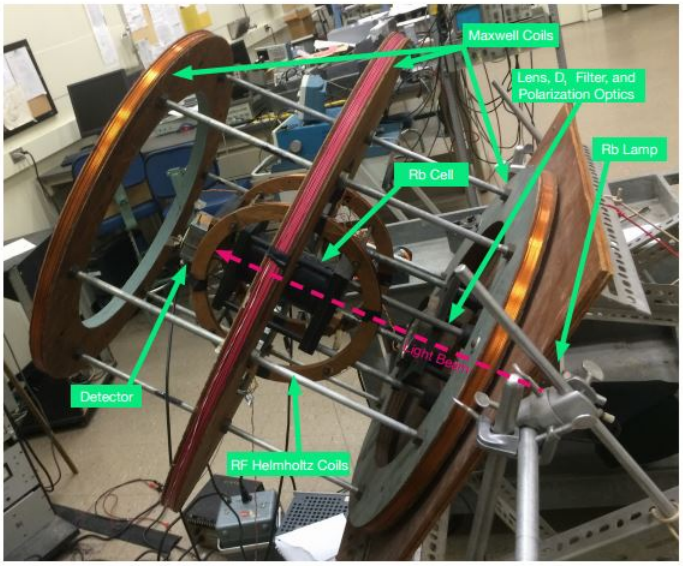

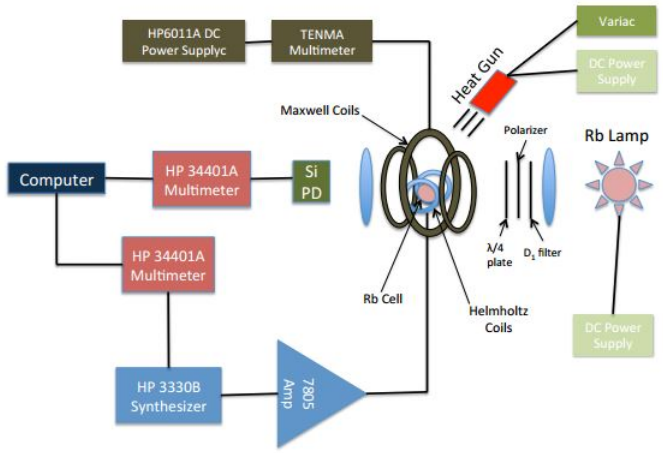

Fig. 2. The Optical pumping apparatus and the basic layout of the experimental setup.

A. Rubidium Cell and Lamp

A Rubidium lamp emits D_1 and D_2 radiation which is collimated, filtered for D_1 light, polarized then passed through a quarter wave plate to obtain radiation with a known helicity. The Rubidium cell contains both Rb^{85} and Rb^{87} with a buffer gas. Light emerging from the Rubidium cell is refocused then hits a Si photodiode. A resistor converts the photodiode current reading into a voltage reading which is read out to a multimeter, and eventually the computer with LabView software.

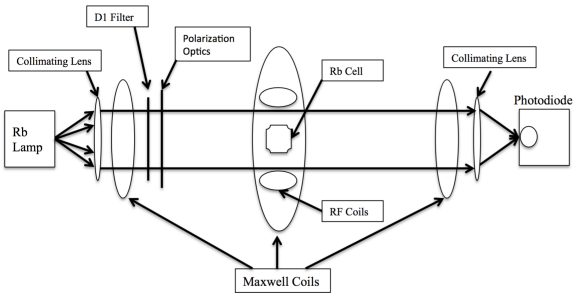

Fig. 3. A diagram of the experimental apparatus. The apparatus is set approximately 30 degrees to the floor. This is to coarsely align the device to the Earth's magnetic field. The dimensions of the apparatus and the magnetic field of the coils are discussed later in the section.

B. Maxwell Coil

The Maxwell coils provide a uniform external magnetic field around the Rubidium cell. The Maxwell coils are driven by a power supply which provides a current to produce a homogeneous magnetic field. In order to provide a highly uniform field around the Rubidium cell, three Maxwell coils are arranged such that the magnetic field produced is parallel or anti-parallel with the "beamline." Two smaller coils (A and C) sandwich a larger coil (B). The B coil is wound with 0.1325cm copper wire, with 142 turns, and a diameter of 78.4cm. At a distance of 26.2cm in both directions along the beamline from the center coil, there two coils (A and C) which are wound with 0.1325cm copper wire, with 110 turns, and a diameter of 59.1cm. The current for the Maxwell coils are supplied by a HP6011A DC Power Supply. The frequency range of the Maxwell Coils are swept by a HP3330B Automatic Synthesizer.

Given a value of supply current, the magnetic field due to the three Maxwell coils can be calculated. The expression below accounts for all three Maxwell coils. The B-Field is given per unit current, so that the magnetic field for a given current is always known:

$$\frac{B_{coil}}{I} = \left(\frac{\mu_0 N_A R_A^2}{(x^2+R_A^2)^{3/2}} + \frac{\mu_0 N_B R_B^2}{2R_B^{3/2}} + \frac{\mu_0 N_C R_C^2}{(x^2+R_C^2)^{3/2}}\right)$$

From this, the external field per unit current was determined to be $2.93 \times 10^{-4} \frac{T}{A}$.

C. Data Acquisition

The radiation from the Rubidium lamp after it has passed through the Rubidium cell is captured by a photodiode, generating a signal. The signal is amplified by a PRD Harris 7805 amplifier. The photodiode signal is read out by a Agilent 34401A DMM, then to the computer where LabView software will record the data. This software has two tabs. THe "Lamp, Cell warm up" is used when we calculate the absorption cross-section wherein it tabulates photodiode voltage and the corresponding temperature of the Rb cell. The "Frequency vs Transmission" tab is used for all other parts of the experiment where it plots photodiode voltage as a function of RF frequency. This is useful is observing the resonance peak.

V. Measurements

A. Absorption Cross-Section

At room temperature, Rubidium is in solid state. Before we begin our experiment, we heat this with a heating coil and a fan for it to be be vaporized. The number density of Rubidium vapor can be expressed by Ideal gas law equation $n = \frac{P}{K_b T}$. Also, the Vapor pressure can be written as a function of temperature [6].

$$log_{10} P = 4.857 - \frac{4215}{T}$$

where P is the pressure expressed in atm and T is the temperature expressed in Kelvin. Combining the above equation gives us

$$n = \frac{10^{4.857 - 4215/T}}{1.38 \times 10^{-23} \times T}$$

The Beer-Lambert's law gives a relation between the transmitance and cross-section.

$$I = I_0 e^{-\sigma n l}$$

where I is transmittance, I_0 is total transmittance, σ is cross-section, n is number density and l is the length of rubidium cell (5cm). As the photo diode voltage is a measure of transmittance, we make our plot photodiode voltage with respect to number density.

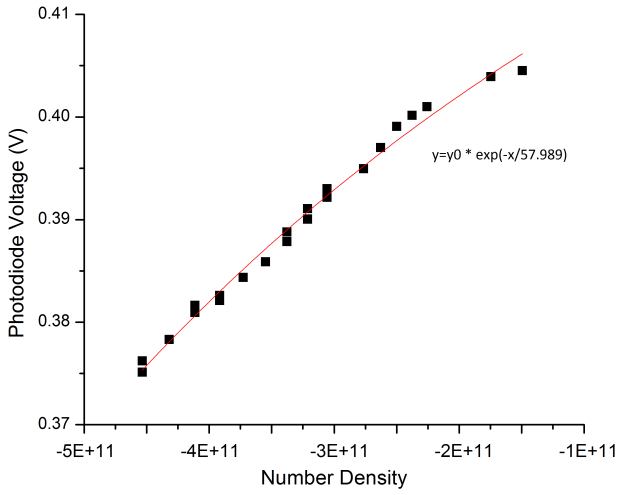

Fig. 4. Absorption cross section - photodiode voltage plotted as a function of number density. It is fitted to an exponential decay fit.

From fitting of the above curve, we obtain $\sigma = 0.569 \times 10^{-16}\ m^2$.

B. Basic resonance curve

When all atoms are in optically pumped state, the light from Rb lamp passes through without absorption. The Helmholtz coil surrounding the magnet sweeps through a wide range of radio-frequency. When the frequency matches the magnetic sublevel frequency, it causes a stimulated emission. Atoms that are now dumped to the lower magnetic sublevels can absorb the D1 line. This is the typical resonance curve.

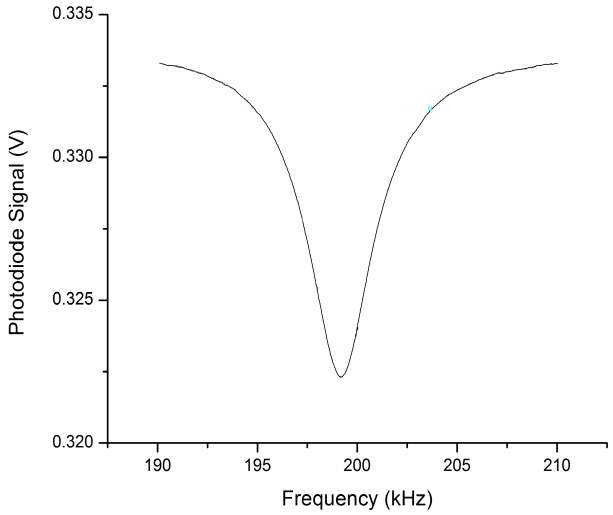

Fig. 5. Simple resonance curve of Rb85. Signal amplitude of -30dB and no external magnetic field provided by Maxwell coils.

The uncertainity in this measurement was calculated by repeating this measurement 20 times and obtaining the mean and the standard deviation for the data set. For ^{85}Rb we obtain, $\nu = 199.490 \pm 0.0505$ kHz.

C. Ambient Magnetic Field and Lande g-factor

Under weak external magnetic field, we obtain the resonance peak and its frequency as $\nu = 199.49 \pm 0.0505\ kHz$ for ^{85}Rb, as obtained from the Fig 5. We substitute this in equation (1) along with theoretical values of all constants. In this case, B_{ext} = B_{earth} + $B_{ambient}$. The value of the magnetic field in Stony Brook is $51.739 \pm 0.152\ \mu T$ [7] . Using this we obtain the value of $B_{ambient} = 46.413 \pm 0.152\ \mu T$.

In part two, we measure the Lande g-factor, this is a measure of how the effective magnetic moment of a bound electron changes due to its interaction with orbital angular moment and the spin of the nucleus. By theoretical calculation we found for F=3, g_f = 1/3 for ^{85}Rb and for F=2, g_f = 1/2 for ^{87}Rb. Here we make a plot of ν vs B, and fit the graph to obtain the g_f.

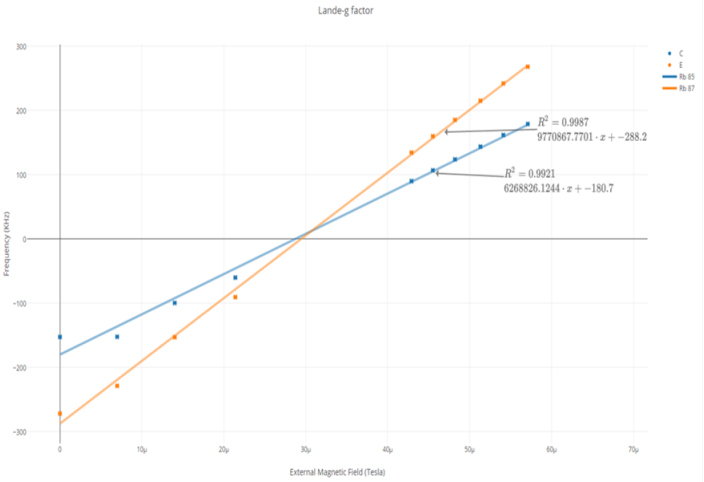

Fig. 6. Center peak frequency as a function of external B-field. Though negative frequency is a non physical measurement, for the sake of fitting data, the left hand side of $B_{total} = 0$ was reflected about the $\nu = 0$, made negative and overall fit linearly to determine the slope.

From the above plot, we obtain the g_f value to be 0.35 ± 0.0071 for ^{85}Rb for F=3 and 0.52 ± 0.0143 for ^{87}Rb for F=2 which are very close to the theoretical value.

D. High B-field regime

In the high B-field regime, the energy splitting of each level would be separated enough for us to see these as different peaks. Given below is the absorption line of ^{85}Rb. As expected we see distinct 7 peaks each corresponding to various sub-magnetic levels of F=3. The frequency at different peaks is tabulated as below:

Transition (Mf ->Mf*)	Frequency (Mhz)
3 -> 2	2.767
2 -> 1	2.772
1 -> 0	2.777
0 -> -1	2.782
-1 -> -2	2.788
-2 -> -3	2.793

Fig. 7. Table showing the frequency values corresponding to stimulated emission due to dumping of electrons to lower level.

All the mentioned frequency have an uncertainty of $\nu = \pm 0.0505$.

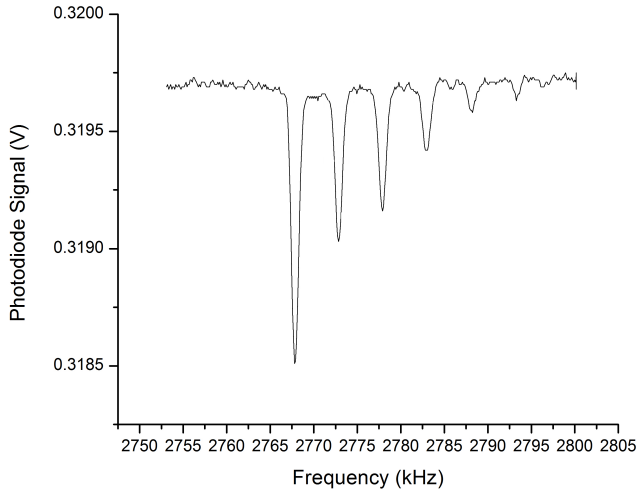

Fig. 8. Figure showing multiple peaks in the high B-field regime. The magnetic field provided by the Maxwell coils are $3.93 \times 10^{-4} T$

There is a monotonic relationship between the frequency of the magnetic field and the hyper-fine excitation states. The first peak corresponds to $M_f = +2 \ to + 1$, and the next corresponds to $M_f = +1 \ to + 0$ etc. Also, the depth of the optical resonance is proportional to the population difference between each pair of Zeeman level that electron gets dumped to. We notice that the population difference between $M_f = +2 \ to + 1$ is much higher than between $M_f = +1 \ to + 0$. This suggests that the optically pumped state is $M_f = +2$, which means the D1 line is $\sigma+$ polarized.

E. Power Broadening

Power Broadening is a term to indicate the change in the width of the resonance peak as the amplitude is changed keeping the range of frequency sweep constant. At various power ratio, we obtained the resonance peak and made a Gaussian fit to this and obtained its full width half maximum (FWHM) value. Given below is a plot of FWHM at various decibel values. We notice that with decreasing power ratio, the width also decreases. As we can see, even when we extrapolate the graph, the width never becomes zero. Another noticeable feature is that the width is always greater for ^{87}Rb than ^{85}Rb. Here, we give an explanation for these two characteristics. Firstly, consider the energy, time uncertainty relation - $\Delta E \Delta t \geq \hbar/2$. We can interpret ΔE as the energy dispersion of a state and Δt as the lifetime of the state itself. Here even at zero attenuation, the width corresponds to the fuzziness around the energy level, that is, there is no one distinct level that the electron can get excited it, but it is a small band of energy level whose width is determined by the lifetime of the electron in that state. Secondly, considering dipole moment of radiation, the power of radiation id proportional to ω^4, thus larger the energy difference between the two levels, more will the width in resonance curve. ^{87}Rb has a larger energy difference between subatomic level than ^{85}Rb.

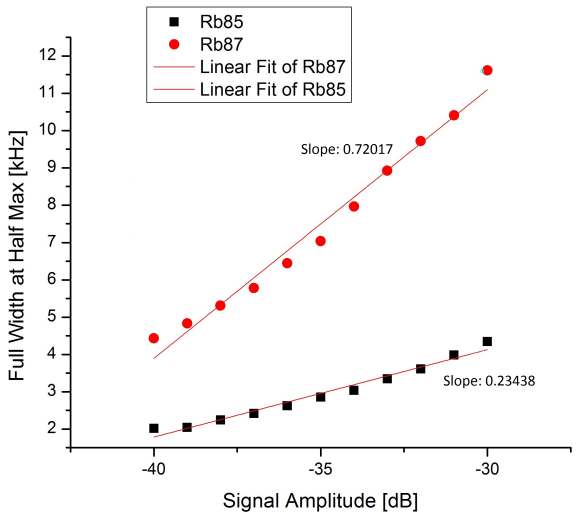

Fig. 9. Full width at half max is shown as a function of power (signal in dB). The slope for the black line (Rb85) was reported to be 0.23438 with an intercept of 11.16 (kHz). The slope of the red line (Rb87) was reported to be 32.70281 with an intercept of 32.70 (kHz).

VI. Conclusion

This simple setup and method of data taking helped us explore some of very fundamental aspects of Quantum Mechanics. It was also a window into the wide world of Atomic physics which neither of us had any experience in. In this section, we summarize some of our main results from doing this experiment.

- We plotted the absorption cross-section of Rubidium atom and obtained the value to be $\sigma = 0.569 \times 10^{-16}\ m^2$. Comparing this with values obtained in the same setup by other lab groups, we realize that we have similar value in the same order of magnitude.
- We calculated the ambient magnetic field and obtained $B_{ambient} = 46.413 \pm 0.152 \mu T$. This could be due to personal electronic equipment and other laboratory setups which uses AC signals or magnetic field. We were surprised at getting such a high value of the magnetic field, which is almost comparable to the Earth's field.
- The value of g_f that we obtained by fitting a linear graph of ν vs B_{ext} is . These agree quite reasonably with the theoretical value.
- In the high B-field regime, we were able to see the 6 peaks of Zeeman splitting for ^{85}Rb and in Fig 7, we tabulated the values obtained from the graph. Also, the structure of the Zeeman splitting indicated that we have a $\sigma+$ D1 line.
- We only have a qualitative understanding of the Power broadening, which gives a linear relationship between the FWHM and signal amplitude. The explanation and understanding of this linear behavior is discussed in the Power broadening sub-section in the context of Energy-Time uncertainty.
  One thing we should have done is uncertainty calculation. We should have taken the basic resonance frequency plot multiple times which would have helped us realize uncertainty in the values obtained from fits. As this value was unknown, we couldn't propagate the errors into other fits and thus compare if the theoretical values fall within it.

VII. Author Contribution

Most of the data acquisition was jointly done by both of us. Specific contributions are mentioned as below:

Niveditha: Abstract, Theoretical Model, Measurements (Analysis using values from plots) and Conclusion.

William: Introduction, Previous works, Experimental setup and all the data plotting for every measurement, data acquistion for uncertainity.

VIII. Acknowledgment

We thank Professor. Eden Figueroa for taking the time to explain the theoretical concepts behind this experiment right in the beginning, which helped us appreciate all the results that we obtained and its significance. We also thank our teaching assistant, Chris Ianzano who assisted us through all the difficulties that the setup caused and helped us obtain the plot for Zeeman splitting.

.

References

[1] $http://www.nobelprize.org/nobel_prizes/physics/laureates/1973/press.html$
[2] $https://en.wikipedia.org/wiki/Josephson_effect$
[3] $https://en.wikipedia.org/wiki/Four-terminal_sensing$
[4] $http://www.wmi.badw.de/teaching/Lecturenotes/AS/AS_Chapter2.pdf$
[5] $https://en.wikipedia.org/wiki/Superconductingtunneljunction$

[6] $http://george.ph.utexas.edu/\ dsteck/alkalidata/rubidium87numbers.pdf$
[7] $WorldMagneticModel, MagneticFieldcalculator, http://www.ngdc.noaa.gov/geomag-web/igrfwmm$
[8] $https://www.hep.wisc.edu/\ prepost/407/opticalpumping/opticalpumping.pdf$
[9] $http://instructor.physics.lsa.umich.edu/adv-labs/Optical_Pumping/OpticalPumping2.pdf$
[10] $https://en.wikipedia.org/wiki/Zeemaneffect$